Magnetospheric injection of ELF/VLF waves with modulated or steered HF heating of the lower ionosphere

M. B. Cohen,[1] U. S. Inan,[1,2] D. Piddyachiy,[1] N. G. Lehtinen,[1] and M. Gołkowski[3]

Received 8 October 2010; revised 7 March 2011; accepted 15 March 2011; published 16 June 2011.

[1] ELF/VLF waves have been generated via steerable HF heating of the lower ionosphere. The temperature-dependent conductivity of the lower ionospheric plasma enables HF heating (and subsequent recovery) to modulate natural current systems such as the auroral electrojet, thus generating an antenna embedded in the ionospheric plasma. We apply a realistic three-dimensional model of HF heating and ionospheric recovery, as well as ELF/VLF wave propagation in and below the ionosphere, to derive the radiation pattern into the magnetosphere as a result of steerable HF heating. It is found that modulated HF heating preferentially directs signals upward into space because of the phasing effect of the upward HF wave propagation. We find that the steering techniques such as the geometric modulation "circle sweep" enhances the total ELF/VLF power injected into the magnetosphere by 5–7 dB compared to amplitude modulated heating, with a few dB enhancement in the peak magnetic field value. Another technique known as beam painting enhances the total injected power by 1–3 dB but produces weaker peak magnetic fields due to the power being spread over a larger area. Observations on the DEMETER spacecraft are presented and compared with theoretical predictions. DEMETER observations show that the signal produced with geometric modulation can be stronger than the signal from AM under the same conditions.

Citation: Cohen, M. B., U. S. Inan, D. Piddyachiy, N. G. Lehtinen, and M. Gołkowski (2011), Magnetospheric injection of ELF/VLF waves with modulated or steered HF heating of the lower ionosphere, *J. Geophys. Res.*, *116*, A06308, doi:10.1029/2010JA016194.

1. Introduction

[2] The space environment surrounding the Earth is strongly influenced by extremely low frequency (300–3000 Hz) and very low frequency (3–30 kHz) radio waves. For instance, global lightning activity radiates intense electromagnetic energy in the ELF/VLF frequency range, which dominates the natural radio environment at these frequencies [*Chrissan and Fraser-Smith*, 1996], some portion of which leaks through the ionosphere in the plasma whistler mode [*Helliwell*, 1965]. These right-hand circularly polarized waves can interact with energetic (>1 keV) radiation belt electrons, inducing particle precipitation onto the ionosphere [*Peter and Inan*, 2007] and/or amplification of the waves. Furthermore, ELF/VLF waves can be generated in situ, in the form of hiss [*Hayakawa and Sazhin*, 1992] or chorus [*Sazhin and Hayakawa*, 1992], as a result of cyclotron-resonant interactions between whistler waves and energetic electrons.

[3] It is therefore useful to conduct controlled wave injection experiments to quantify the role of ELF/VLF waves in radiation belt dynamics. Unfortunately, it is difficult to generate ELF/VLF waves due to their extremely long wavelengths (10–1000 km), making a practically realizable vertical mast antenna too short, while a long horizontal antenna is hindered by image currents from the conducting ground.

[4] At Siple Station, Antarctica, a 21 km long horizontal crossed-dipole VLF transmitter was constructed on top of a 1–2 km thick ice sheet, which effectively lifted the antenna off the conducting ground [*Raghuram et al.*, 1974]. Controlled injection of whistler mode signals into the magnetosphere and excitation of triggered nonlinear emissions were regularly observed both at Siple and at the geomagnetic conjugate point in Northeastern Canada [*Helliwell*, 1988].

[5] Since the HF waves modify the conductivity of the lower ionosphere (i.e., 60–100 km altitude), ON-OFF modulation of the HF power at ELF/VLF waves can modulate natural currents passing through the ionosphere, such as the auroral electrojet, thereby turning the lower ionosphere into a large antenna. ELF/VLF generation in this manner was achieved first in Gorky (now Nizhny Novgorod), Russia [*Getmantsev et al.*, 1974] and then more extensively in Tromsø, Norway [*Stubbe et al.*, 1981]. The high-power auroral stimulation (HIPAS) facility was later

[1] STAR Laboratory, Department of Electrical Engineering, Stanford University, Stanford, California, USA.
[2] Department of Electrical Engineering, Koc University, Sariyer-Istanbul, Turkey.
[3] Department of Electrical Engineering, University of Colorado Denver, Denver, Colorado, USA.

0148-0227/11/2010JA016194

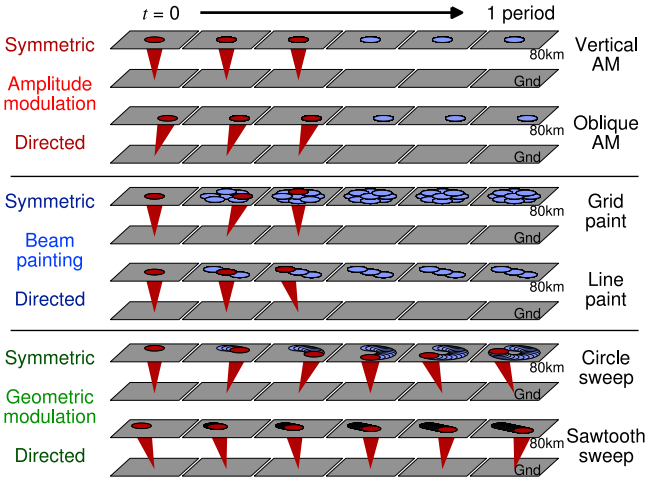

Figure 1. Schematic view of six forms of HF modulation, amplitude modulation, beam painting, and geometric modulation, each implemented in a symmetric or directed form.

built near Fairbanks, Alaska, and utilized for ELF/VLF wave injection [*Ferraro et al.*, 1989] until 2009. The latest of these "HF heater" facilities, the High Frequency Active Auroral Research Program (HAARP) facility, was constructed near Gakona, Alaska (62° 22′N, 145° 9′W), and utilized for ELF/VLF wave generation first in an earlier developmental stage [*Milikh et al.*, 1999] and then in an upgraded stage [*Cohen et al.*, 2008a] utilizing 3.6 MW of HF power and effective radiated power (ERP) up to 3800 MW. HAARP generated ELF/VLF signals have been observed as far as 4400 km along the Earth-ionosphere waveguide [*Moore et al.*, 2007; *Cohen et al.*, 2010c].

[6] A number of workers have discussed the magnetospherically injected signal from modulated HF heating, using satellite observations as well as theoretical models. *James et al.* [1984] observe ELF/VLF radiation from Tromsø on the ISIS-1 satellite and compare to simultaneous ground measurements. *James et al.* [1990] subsequently observe signals with the DE-1 spacecraft, and discuss the harmonic content of the received signal, spectral broadening and propagation delays. *Lefeuvre et al.* [1985] observe ELF/VLF signals on the Aureol-3 satellite from the Tromsø facility. *Kimura et al.* [1991, 1994] observe signals from HIPAS and Tromsø, respectively. *Yagitani et al.* [1994] construct a theoretical model of the radiation to LEO altitudes, with *Nagano et al.* [1994] then presenting an experiment at HIPAS with accompanying theoretical calculations.

[7] The HAARP facility has also been used to generate ELF/VLF waves observed aboard satellites [*Platino et al.*, 2004, 2006; *Piddyachiy et al.*, 2008]. Due in large part to its location just inside the plasmapause, HAARP is the first HF heating facility that has been able to generate ELF/VLF signals that are amplified by gyroresonant wave-particle interactions in the radiation belt [*Inan et al.*, 2004; *Gołkowski et al.*, 2008], in a manner similar to the earlier observation at Siple Station. However, recent comparisons between amplified signals observed from Siple and HAARP indicate that HAARP-generated signals in the magnetosphere are close to the threshold for nonlinear amplification and subsequent generation of triggered emissions [*Gołkowski et al.*, 2009], even when magnetospheric conditions are favorable for amplification.

[8] There have also been some recent efforts to boost the amplitudes of generated ELF/VLF signals at HAARP using HF beam steering, as opposed to amplitude modulated HF heating that has been utilized in many experiments to date. Figure 1 shows a schematic view of six forms of modulation including HF beam steering, reflected in the six rows. Each row shows six snapshots of the HF beam position during the ELF/VLF period, with the ground and ionosphere with gray planes. The top two rows depict amplitude modulation, where the beam remains in a fixed direction, ON for the first half of the period, and OFF for the second half of the period. The amplitude modulation can be implemented in two forms, a symmetric form (vertical AM, where the beam is vertically oriented, depicted in the first row), or a directed form (oblique AM, where the beam is pointed at an angle, depicted in the second row). The middle two rows depict beam painting (first proposed by *Papadopoulos et al.* [1989]), where the ON portion is accompanied with rapid beam motion. The beam painting can be implemented in a symmetric form (grid paint, where the beam locations are azimuthally uniform, shown in the third row) and a directed form (line paint, where the beam locations are aligned along an azimuth, shown in the fourth row). The bottom two rows depict geometric modulation, where the HF beam remains ON but moves slowly in a geometric pattern. Geometric modulation can be implemented in a symmetric form (circle sweep, where the beam sweeps in a circular shape, as in the fifth row) or a directed form (sawtooth sweep, where the beam sweeps one direction along an azimuth, as shown in the sixth row).

[9] Experimental and theoretical results regarding the injection of ELF/VLF waves into the Earth-ionosphere waveguide and observed on the ground from steered HF heating have been previously presented [*Cohen et al.*, 2008b, 2010b, 2010a]. However, the signal injected in the magnetosphere may not be accurately assessed by measurements on the ground, since the two may be poorly or even negatively correlated. Unfortunately, continuous satellite observations of fields entering the magnetosphere are impossible. In this paper, we turn to a theoretical model to characterize the injection of ELF/VLF wave energy into the magnetosphere, as a function of ELF/VLF frequency and beam modulation technique, and present some limited satellite observations for comparison.

2. Magnetospheric Injection With HAARP

[10] The theoretical model utilized is identical to that described by *Cohen et al.* [2010a], using similar physical principles from past works [*Tomko*, 1981; *James*, 1985; *Rietveld et al.*, 1986; *Moore*, 2007; *Payne*, 2007]. The HF heating model steps forward in small time steps and solves an energy balance equation in a three-dimensional space to calculate the HF absorption, modified electron temperature, modified collision frequency, and modified ionospheric conductivity tensor, with the remaining HF energy propagated upward. The electron temperature distribution is assumed to remain Maxwellian, and the electron density is assumed to remain constant. Once sinusoidal steady state is established, the modified conductivity at each location is

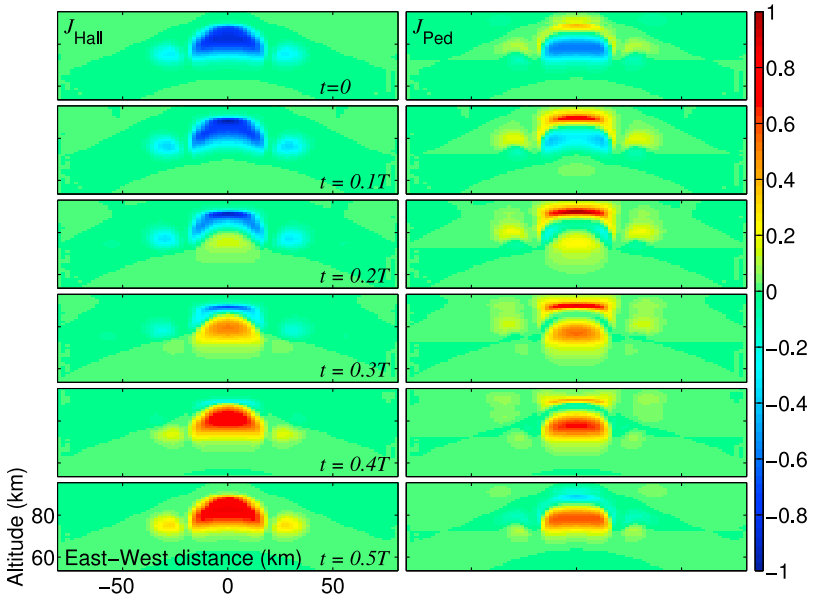

Figure 2. Variation of the (left) Hall and (right) Pedersen currents from 3 kHz vertical AM heating at 3.25 MHz at 6 points in the ELF/VLF cycle. The 3 kHz Fourier-extracted currents all vary sinusoidally with some amplitude and phase.

tracked in time, and the Fourier component at the modulation frequency is extracted. A realistic HAARP HF radiation pattern and geomagnetic field are used, along with a typical winter daytime ionosphere derived from the International Reference Ionosphere, and the electron density extrapolated to lower altitudes with exponential decay.

[11] Figure 2 shows the evolution of the modulated currents (at the 3 kHz fundamental frequency and vertical AM heating at 3.25 MHz) over an ELF/VLF period (T), taking into account both the phase of the Fourier-extracted conductivity waveform, and the delay from the HF propagation from the ground through the ionosphere. Figure 2 (left) shows a vertical slice of the Hall currents and (right) the Pedersen currents. The panels show frames spaced out at six times during the ELF/VLF period. Heating from both the main beam, and side lobes, can be observed.

[12] The upward propagation of the HF produces a vertical phase gradient to the modulated currents such that the current structure appears to be moving upward at nearly the speed of light. This traveling wave effect may contribute to the formation of the "column" of radiation (described by *Payne et al.* [2007], *Piddyachiy et al.* [2008], and *Lehtinen and Inan* [2008]), and indicates an advantage of HAARP HF heating for the purpose of magnetospheric injection that is not possible with a conventional ELF/VLF transmitters such as that once present at Siple Station. At the same time, the vertical phase gradient may act to limit the signal strength injected into the Earth-ionosphere waveguide, by preferentially directing signals upward.

[13] Since the vertical phase gradient is dominated by the propagation of the HF waves, which is close to the speed of light in the D region, the preferential injection into space is not a strong function of ELF/VLF frequency. It should also be noted that because the polarity of the Pedersen conductivity changes turns over in the heated region, the vertical phase gradient is predominantly associated with the Hall currents. However, past experiments (and simulations shown in Figure 3) indicate the Hall currents are likely the dominant generator of ELF/VLF waves with HF heating.

[14] The Fourier-extracted conductivity variations act as AC current sources assuming a constant electrojet field of 10 mV/m, oriented to geomagnetic north. Although the electrojet value in practice can vary substantially, the electric field simply scales the radiated electromagnetic pattern accordingly, so considering a fixed value of ambient electrojet has no effect on the results here.

[15] The calculated sources are used to drive a model of Earth-ionosphere wave propagation described in detail by

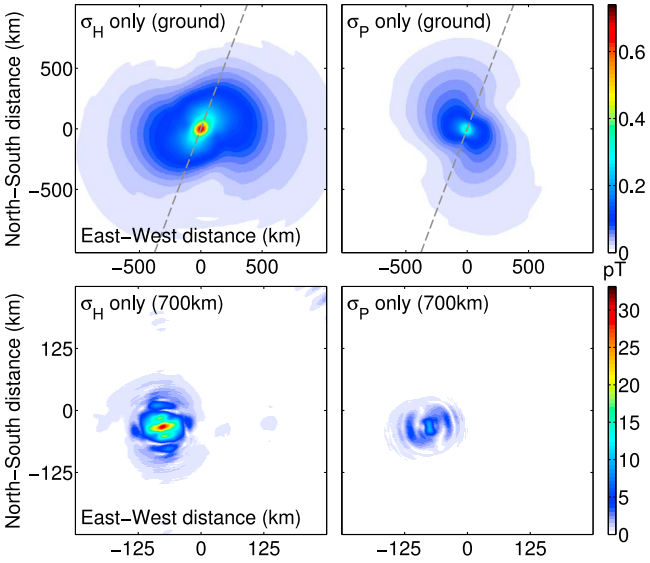

Figure 3. The magnetic field radiation pattern resulting from the (left) Hall and (right) Pedersen currents on the (top) ground and at (bottom) 700 km altitude.

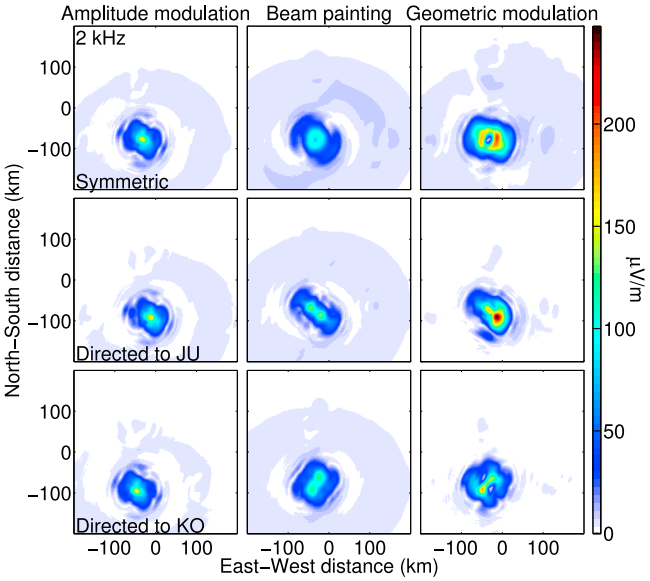

Figure 4. The modeled radiation pattern at 700 km resulting from the nine methods of generation at 2 kHz and 3.25 MHz.

Lehtinen and Inan [2008, 2009]. It takes advantage of Snell's law in the plane-stratified medium to calculate the electromagnetic field for each horizontal wave vector component $\mathbf{k}_\perp$ in the Fourier decomposition over horizontal coordinates $\mathbf{r}_\perp$. At each $\mathbf{k}_\perp$, the reflection coefficients and mode amplitudes are calculated recursively in a direction which provides stability against the numerical "swamping" which is inherent in many similar methods [*Budden*, 1985, pp. 574–576]. The configuration space field is obtained by taking the inverse Fourier transform $\mathbf{k}_\perp \rightarrow \mathbf{r}_\perp$. The method can treat arbitrary harmonically varying sources by applying appropriate boundary conditions between the strata of the medium. The values of $\mathbf{k}_\perp$ for field calculations are taken at grid points on an optimized mesh. The electromagnetic fields, below, within, and above the ionosphere are simultaneously calculated. The magnetic field and ionosphere are assumed to be homogeneous in the horizontal direction, which is roughly true at high latitudes up to 700 km.

[16] We calculate the generated fields up to an altitude of 700 km, which is located at the topside of the ionosphere, where the DEMETER satellite orbits. We note, however, that the propagation model does not take into account irregularities in the ionosphere, particularly those which may be present due to the HAARP HF heating effects in the *E* and *F* region of the ionosphere. Such irregularities may be responsible for a significant disparity between theoretical amplitudes of VLF signals in the magnetosphere, and those observed by satellites [*Starks et al.*, 2008; *Lehtinen and Inan*, 2009].

[17] Figure 3 shows the radiation pattern from σ_H and σ_P currents, separately, for 3.25 MHz, vertical AM 2 kHz heating. Figure 3 (top) shows the predicted horizontal magnetic fields on the ground, up to 1000 km distance from HAARP. The gray line shows the geomagnetic north-south direction (and the direction of the electrojet fields). Figure 3 (bottom) shows the radiation at 700 km altitude, up to 250 km laterally from the HF array.

[18] This decoupling enables comparison of the contributions of the Hall and Pedersen conductivities, for both Earth-ionosphere and magnetospheric injection. In this case, it appears that the Hall conductivity produces stronger ELF/VLF radiation, whereas the Pedersen conductivity contributes a smaller amount to the radiated ELF/VLF pattern. The upward ELF/VLF radiation remains tightly bound to the field line, as discussed by *Lehtinen and Inan* [2008].

3. Comparison of HF Beam Techniques

[19] We now apply the model in order to compare the magnetospheric injection of amplitude modulation, beam painting, and geometric modulation.

[20] The simulated beam motion speed is an important parameter in these simulations (as they are in experiments). In the beam painting simulations, the beam dwell time is simulated at 2 μs. Although this is shorter than HAARP is currently capable of performing, it reflects a more ideal implementation of beam painting, since the cycle through nine beam locations (18 μs) is still well shorter than the VLF period at 10 kHz. Furthermore, the 18 μs cycle time is substantially shorter than both the electron temperature saturation time (a few hundred μs) and the electron temperature recovery time (several hundreds of μs). However, because the electron temperature recovers slower than it heats, heating a given ionospheric location with occasional short pulses results in only a minimal loss of effectiveness (as described by *Papadopoulos et al.* [1989] and quantified by *Cohen et al.* [2010a]).

[21] In the geometric modulation techniques, the beam sweep rate depends on the ELF/VLF period, since the beam sweep takes exactly one ELF/VLF period to complete. The beam sweep was carried out with 20 equal length steps. In the circle sweep at 3.25 MHz, approximately 20% of the total area is being heated at a given time, so the beam dwell time on a location lies between ~25 and 400 μs, depending on ELF/VLF period between 500 Hz an 7500 Hz.

[22] Figure 4 shows the horizontal magnetic field from 2 kHz modulated heating, 3.25 MHz. The three columns correspond to amplitude modulation (Figure 4, left), beam painting (Figure 4, middle), and geometric modulation (Figure 4, right). The three rows show the symmetric implementation (Figure 4, top), directed implementation toward the southeast, and directed implementation toward the southwest, as shown in Figure 1. The null in the center of the circle sweep (Figure 4, top right) is consistent with the unheated spot in the center as the beam traverses a circle.

[23] These simulations are repeated between 500 Hz and 9.5 kHz, in 500 Hz increments, plus 250 Hz, and the results shown in Figure 5. The total power injected into the magnetosphere is determined by calculating the Poynting vector ($\vec{E} \times \vec{H}$, where $\mu\vec{H} = \vec{B}$) at each location, and plotted in Figure 5 (left). The upward component of the Poynting vector gives the power density in the vertical direction, which can be integrated over a plane at 700 km altitude.

[24] Common to all the beam motion techniques is a substantial drop in power injected into the magnetosphere with increasing frequency between 1 and 9.5 kHz. This effect is intrinsic to HF heating of the ionosphere, and not related to the beam motion techniques. For instance, mea-

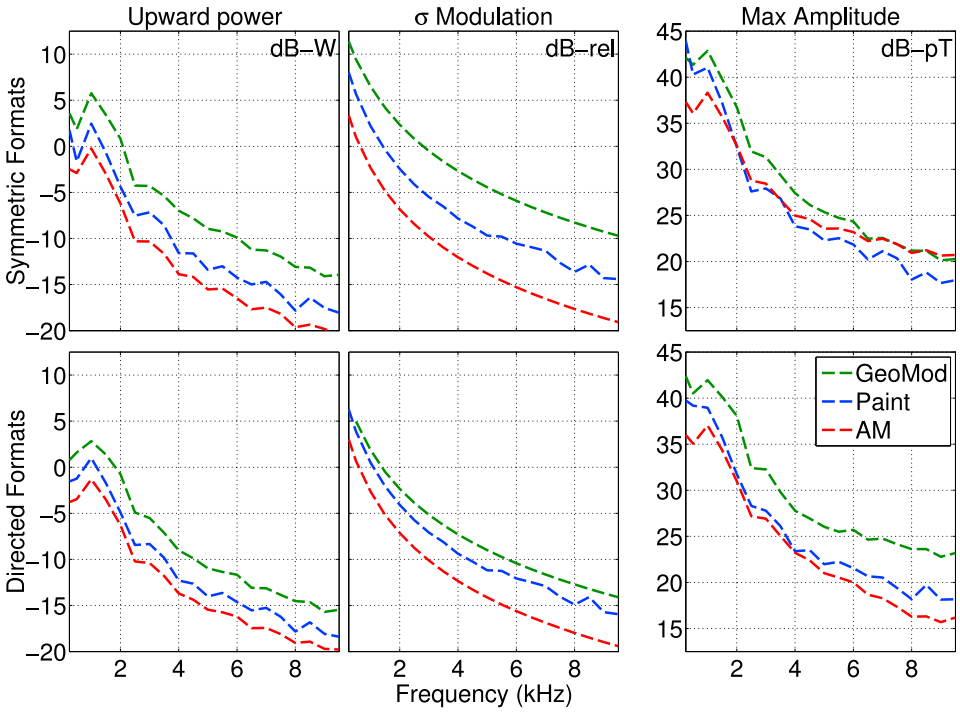

Figure 5. (left) Total power, (middle) total L2 norm conductivity modulation, and (right) maximum magnetic field amplitude as a function of ELF/VLF frequency and modulation technique. (top) Symmetric and (bottom) directed formats (in this case to the southwest).

surements on the ground (in the near field) of efficiency as a function of ELF/VLF frequency indicate a maximum around 2 kHz, with reductions in efficiency both above and below, after accounting for waveguide effects [*Rietveld et al.*, 1986, 1989]. Above this maximum efficiency frequency, the on and off modulation occurs too quickly for the electrons to respond (since the recovery rate is some hundreds of μs). This same effect applies to magnetospheric injection, as well, and is clearly visible in Figure 5, in the weakening injected power for higher frequencies.

[25] The effect of heating efficiency as a result of saturation time can be seen by separately plotting the integrated conductivity modulation, which is simply the sum of all the total conductivities at all grid points (arbitrarily scaled), where 'total conductivity' refers to the L2 norm of the Hall and Pedersen conductivity. As shown in Figure 5 (middle), the integrated conductivity continues to increase below 1 kHz (due to contributions from slowly recovering portions at the highest altitudes), in contrast to the calculated magnetospheric power.

[26] Ground measurements taken in the near field indicate, at <500 Hz, substantially lower magnetic fields compared to the peak [*Rietveld et al.*, 1986; *Papadopoulos et al.*, 2005]. Theoretical models either overpredict or underpredict the magnetic fields at <500 Hz, depending on whether secondary currents in the ionosphere are included or ignored, respectively [*Rietveld et al.*, 1989]. The full wave model utilized here ignores secondary currents.

[27] For the magnetospheric injection, unlike the ground measurements, as the frequency drops below 2 kHz, the modeled magnetospheric injection continues to rise until ~1 kHz, before leveling off or only modestly declining as far as 250 Hz. Since these calculations are made for 700 km altitude, where the radiated electromagnetic fields dominate, both the near-field and waveguide effects are less important.

[28] The frequency response does show slight but noticeable local maximums at odd multiples of 1 kHz, and local minimums at even multiples of 1 kHz. The opposite effect is generally observed on the ground [*Stubbe et al.*, 1981] and is presumed to be due to Earth-ionosphere cavity resonance effects, since the height of the waveguide, ~75 km, is a half wavelength long at ~2 kHz. This cavity resonance effect therefore has an opposite effect on the magnetospheric injection, with frequencies in between the resonances generating more leakage through the ionosphere.

[29] To compare the various beam techniques, we consider the differences between the curves at each frequency, rather than their overall frequency dependence. For the symmetric implementations (top row), geometric modulation injects 5–7 dB more power into the magnetosphere, but this amplitude enhancement is consistent across all frequencies, unlike the ground-based experimental and theoretical results [*Cohen et al.*, 2010b, 2010a]. Beam painting also appears to yield a smaller (<3 dB) boost in the total power injected into the magnetosphere, compared to amplitude modulation. Although the simulations are repeated for the directed formats (middle and lower rows), the results are not substantially different, unlike the ground-based results which were sensitive to the directionality of the formats.

[30] The maximum magnetic field at 700 km is also shown in Figure 5 (right), since wave injection for the purpose of nonlinear amplification in the magnetosphere may be limited by a threshold wave magnetic field

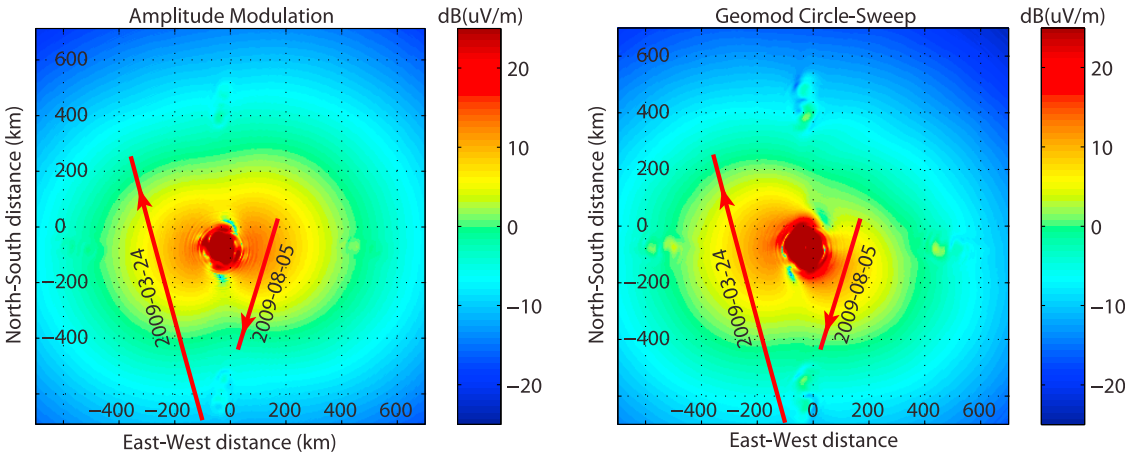

Figure 6. Geometry of two DEMETER passes for which observations are compared to modeling results. (left) Distribution of a horizontal *E* field component at 700 km when amplitude modulation is used. (right) The same for geometric modulation.

[*Helliwell and Inan*, 1982]. For both symmetric and directed formats, geometric modulation produces slightly (few dB) stronger peak magnetic field values compared to amplitude modulation, whereas beam painting produces several dB weaker peak magnetic field values.

4. Satellite Observations

[31] One of the advantages of applying the theoretical model is that observations of magnetospheric injection are much more difficult to acquire. Ground-based receivers can be operated continuously, in a fixed location, whereas orbiting low Earth orbiting (LEO) satellites make only occasional and brief passes over an area, and move rapidly (many km per second) during these passes.

[32] Nevertheless, we can compare the relative amplitudes of AM and geometric modulation observed by the DEMETER satellite as it passes over the HAARP region, to the predicted amplitudes from the model. Figure 6 shows the path of two DEMETER passes, overlaid on top of the distribution of horizontal *E* field at 700 km calculated from the described model for vertical AM (Figure 6, left) and circle sweep (Figure 6, right). The pass on 2009 March 24 is a northbound nighttime pass from 06:52:41 to 06:54:54 UT. The pass on 5 August 2009 is a southbound daytime pass from 20:22:29 to 20:23:36 UT. The chosen passes have reasonably good signal-to-noise ratio and come somewhat close to HAARP, although DEMETER does not pass over the column of high signal, meaning predicted fields are ~30 dB below the maximum in the column.

[33] During these passes, both vertical AM and the circle sweep were alternated with 1 second tones at 1 kHz every 6 seconds. Each experimental point represents 1 s average of filtered 1 kHz narrowband signal from HAARP. This signal was initially identified visually on spectrograms and data points for which noise was higher than the signal were removed from the analysis (e.g., on 24 March 2009 at the distance around 370 km). This means that the variability of the signal at 700 km altitude which is seen from plots is due to the propagation through the ionosphere and not due to the interference with a natural noise.

[34] Although we cannot know the electrojet field strengths in order to make an absolute comparison of the electric and magnetic fields, we can scale the theoretical predictions to roughly match and then look at the relative amplitudes of vertical AM and circle sweep. The relative strengths of vertical AM and circle sweep of horizontal *E* fields along two passes from theory and observations are directly compared in Figure 7. Comparison shows that the theory can approximately predict the position of the region with higher signal. However, the instantaneous values can vary by several times, especially visible on the 24 March 2009 pass, and this cannot be reproduced in the current theory. This variability may result from ionospheric plasma density irregularities, either natural or HAARP-generated. The irregularities may have strong horizontal variation in density and can guide or attenuate waves. In the considered model of the ionosphere any horizontal plasma density structure is neglected. We can also see that at daytime in case on 5 August 2009 the irregularities are probably not as strong and the model predictions are much more accurate.

[35] The comparison between AM and geomod does, however, largely match model results, since both the observed and predicted circle sweep amplitudes near the closest point of the pass are higher than that of amplitude modulation, by a similar amount. It should be noted that some of the disparity between observed and predicted may be due to fluctuations in electrojet strength, since the satellite pass takes a few minutes, over which time span the electrojet strength can vary.

[36] Additionally, from observations we can see that for regions with low variability the difference between vertical AM and circle sweep is small, with only minor dominance of the circle sweep signal. However, for regions with irregularities, the circle sweep signal is substantially higher than vertical AM in several data points. This tendency has also been noted in other cases and need to be studied further, but could result from the lower duty cycle associated with the circle sweep, which may suppress the formation of irregularities.

[37] Finally, we note that the observations presented here are not taken in the so-called "column" of radiation ex-

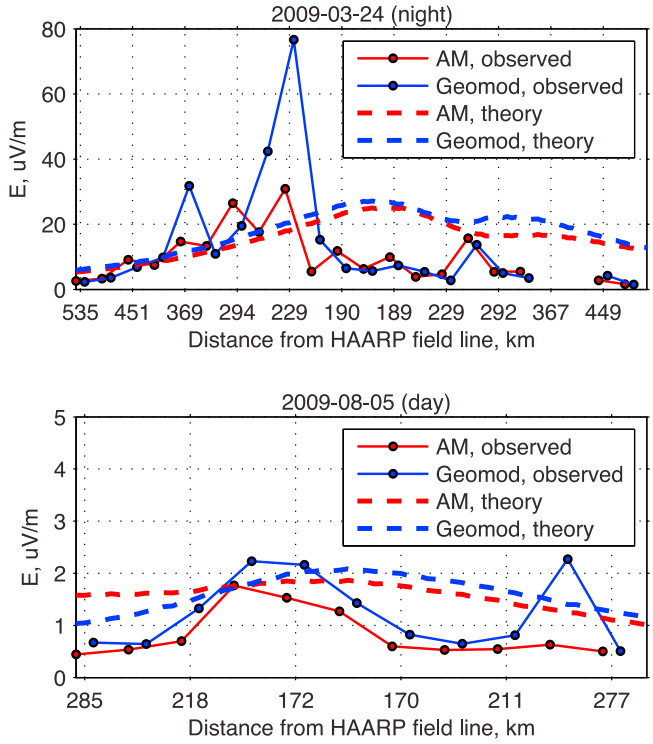

Figure 7. Comparison of theoretical and observational field strengths along two DEMETER passes presented in Figure 6.

tending upward from the heated region (~30 km in diameter). Satellite passes that go through the column are rare and thus associated signals are not yet observed. However, theoretically, since the heated region associated with geometric region is much larger than amplitude modulation, the column itself should be equally widened, contributing to the stronger total ELF/VLF power injected into the magnetosphere from geometric modulation.

5. Conclusion

[38] By applying a theoretical model of HF heating, and ELF/VLF wave propagation, we have predicted, for the first time, the radiation pattern into space resulting from amplitude modulation, beam painting, and geometric modulation of an HF heating beam, as a function of frequency.

[39] The spatial distribution of the radiation pattern appears to be substantially different between theoretical calculations and observations from DEMETER, likely due to horizontal inhomogeneities in the ionosphere that are not accounted for in the ELF/VLF propagation model. It is thus clear that the predicted radiation patterns should only be taken as a general guide of ELF/VLF radiation into the magnetosphere.

[40] Nonetheless, comparison with actual satellite passes confirm the general trend that circle sweep HF modulation produces more ELF/VLF radiation into space compared to amplitude modulation, although the observations here are very limited. It thus appears evident that the circle sweep may be superior for the purpose of magnetospheric injection with HF heating of the ionosphere.

[41] It should also be noted that some observations have also been made of two-hop echoes using amplitude modulation, beam painting, and circle sweep, during times when magnetospheric conditions were appropriate for amplification, and these indicate that the circle sweep produces stronger and more frequent triggered emissions [*Gołkowski*, 2009, pp. 51–54] compared to both amplitude modulation and beam painting. Although this may be in part due to the larger area of the ionosphere subtended by the circle sweep compared to vertical AM, which improves coupling to ducts, it may also be in part due to more ELF/VLF energy entering the magnetosphere from the circle sweep.

[42] **Acknowledgments.** We acknowledge support from HAARP, the Office of Naval Research (ONR), Air Force Research Laboratory (AFRL), and Defense Advanced Research Programs Agency (DARPA), via ONR grant N00014-09-1 and N00014-05-1-0854 to Stanford University. We thank Mike McCarrick, David Seafolk-Kopp, and Helio Zwi for operation of the HAARP array.

[43] Robert Lysak thanks Konstantinos Papadopoulos and another reviewer for their assistance in evaluating this paper.

References

Budden, K. G. (1985), *The Propagation of Radio Waves: The Theory of Radio Waves of Low Power in the Ionosphere and Magnetosphere*, Cambridge Univ. Press, New York.

Chrissan, D. A., and A. C. Fraser-Smith (1996), Seasonal variations of globally measured ELF/VLF radio noise, *Radio Sci.*, *31*(5), 1141–1152.

Cohen, M. B., M. Gołkowski, and U. S. Inan (2008a), Orientation of the HAARP ELF ionospheric dipole and the auroral electrojet, *Geophys. Res. Lett.*, *35*, L02806, doi:10.1029/2007GL032424.

Cohen, M. B., U. S. Inan, and M. Gołkowski (2008b), Geometric modulation: A more effective method of steerable ELF/VLF wave generation with continuous HF heating of the lower ionosphere, *Geophys. Res. Lett.*, *35*, L12101, doi:10.1029/2008GL034061.

Cohen, M. B., U. S. Inan, M. Gołkowski, and N. G. Lehtinen (2010a), On the generation of ELF/VLF waves for long-distance propagation via steerable hf heating of the lower ionosphere, *J. Geophys. Res.*, *115*, A07322, doi:10.1029/2009JA015170.

Cohen, M. B., U. S. Inan, M. Gołkowski, and M. J. McCarrick (2010b), ELF/VLF wave generation via ionospheric HF heating: Experimental comparison of amplitude modulation, beam painting, and geometric modulation, *J. Geophys. Res.*, *115*, A02302, doi:10.1029/2009JA014410.

Cohen, M. B., U. S. Inan, and E. P. Paschal (2010c), Sensitive broadband ELF/VLF radio reception with the AWESOME instrument, *IEEE Trans. Geosc. Remote Sens.*, *48*(1), 3–17, doi:10.1109/TGRS.2009.2028334.

Ferraro, A. J., H. S. Lee, T. W. Collins, M. Baker, D. Werner, F. M. Zain, and P. Li (1989), Measurements of extremely low frequency signals from modulation of the polar electrojet above Fairbanks, Alaska, *IEEE Trans. Antennas Propag.*, *37*(6), 802–805.

Getmantsev, C. G., N. A. Zuikov, D. S. Kotik, N. A. Mironenko, V. O. Mityakov, Y. A. Rapoport, V. Y. Sazanov, V. Y. Trakhtengerts, and V. Y. Eidman (1974), Combination frequencies in the interaction between high-power short-wave radiation and ionsopheric plasma, *Sov. Phys. JETP, Engl. Transl.*, *20*, 101–102.

Gołkowski, M. (2009), Magnetospheric wave injection by modulated HF heating of the auroral electrojet, Ph.D. thesis, Stanford Univ., Stanford, Calif.

Gołkowski, M., U. S. Inan, A. R. Gibby, and M. B. Cohen (2008), Magnetospheric amplification and emission triggering by ELF/VLF waves injected by the 3.6 MW HAARP ionospheric heater, *J. Geophys. Res.*, *113*, A10201, doi:10.1029/2008JA013157.

Gołkowski, M., U. S. Inan, and M. B. Cohen (2009), Amplitude and phase of nonlinear magnetospheric wave growth excited by the HAARP HF heater, *J. Geophys. Res.*, *114*, A00F04, doi:10.1029/2009JA014610.

Hayakawa, M., and S. S. Sazhin (1992), Mid-latitude and plasnaspheric hiss: A review, *Planet. Space Sci.*, *40*(10), 1325–1338.

Helliwell, R. A. (1965), *Whistlers and Related Ionospheric Phenomena*, Dover, Mineola, N.Y.

Helliwell, R. A. (1988), VLF wave-injection experiments from Siple Station, Antarctica, *Adv. Space Res.*, *8*(1), 279–289.

Helliwell, R. A., and U. S. Inan (1982), VLF wave growth and discrete emission triggering in the magnetosphere: A feedback model, *J. Geophys. Res.*, *87*(A5), 3537–3550.

Inan, U. S., et al. (2004), Multi-hop whistler-mode ELF/VLF signals and triggered emissions excited by the HAARP HF heater, *Geophys. Res. Lett.*, *31*, L24805, doi:10.1029/2004GL021647.

James, H. (1985), The ELF spectrum of artificially modulated D/E-region conductivity, *J. Atmos. Terr. Phys.*, *47*(11), 1129–1142.

James, H., U. S. Inan, and M. T. Rietveld (1990), Observations on the DE-1 spacecraft of ELF/VLF waves generated by an ionospheric heater, *J. Geophys. Res.*, *95*(A8), 12,187–12,195.

James, H. G., R. L. Dowden, M. T. Rietveld, P. Stubbe, and H. Kopka (1984), Simultaneous observations of ELF waves from an artificially modulated auroral electrojet in space and on the ground, *J. Geophys. Res.*, *89*(A3), 1655–1666.

Kimura, I., A. Wong, B. Chouinard, T. Okada, M. Mccarrick, I. Nagano, K. Hashimoto, R. Wuerker, M. Yamamoto, and K. Ishida (1991), Satellite and ground observations of HIPAS VLF modulations, *Geophys. Res. Lett.*, *18*(2), 309–312.

Kimura, I., P. Stubbe, M. T. Rietveld, R. Barr, K. Ishida, Y. Kasahara, S. Yagitani, and I. Nagano (1994), Collaborative experiments by Akebono satellite, Tromsø ionospheric heater, and European incoherent scatter radar, *Radio Sci.*, *29*(1), 23–37.

Lefeuvre, J. F., et al. (1985), Detection from Aureol-3 of the modulation of auroral electrojet by HF heating from ELF signals in the upper ionosphere above Tromsø, in *Results of the Arcad* 3 *Project and of the Recent Programmes in Magnetospheric and Ionospheric Physics*, pp. 609–616, Cepedues, Toulouse, France.

Lehtinen, N. G., and U. S. Inan (2008), Radiation of ELF/VLF waves by harmonically varying currents into a stratified ionosphere with application to radiation by a modulated electrojet, *J. Geophys. Res.*, *113*, A06301, doi:10.1029/2007JA012911.

Lehtinen, N. G., and U. S. Inan (2009), Full-wave modeling of transionospheric propagation of VLF waves, *Geophys. Res. Lett.*, *36*, L03104, doi:10.1029/2008GL036535.

Milikh, G. M., K. Papadopoulos, M. McCarrick, and J. Preston (1999), ELF emission generated by the HAARP HF-heater using varying frequency and polarization, *Izv. Vyssh. Uchebn. Zaved Radiofiz.*, *42*(8), 728–735.

Moore, R. C. (2007), ELF/VLF wave generation by modulated HF heating of the auroral electrojet, Ph.D. thesis, Stanford Univ., Stanford, Calif.

Moore, R. C., U. S. Inan, T. F. Bell, and E. J. Kennedy (2007), ELF waves generated by modulated HF heating of the auroral electrojet and observed at a ground distance of ~4400 km, *J. Geophys. Res.*, *112*, A05309, doi:10.1029/2006JA012063.

Nagano, I., K. Miyamura, S. Yahitani, I. Kimura, T. Okada, K. Hashimoto, and A. Y. Wong (1994), Full wave calculation method of VLF wave radiated from a dipole antenna in the ionosphere-analysis of joint experiment by HIPAS and Akebono satellite, *Electr. Commun. Jpn., Part I*, *77* (11), 615–624.

Papadopoulos, K., A. S. Sharma, and C. L. Chang (1989), On the efficient operation of a plasma ELF antenna driven by modulation of ionospheric currents, *Comments Plasma Phys. Controlled Fusion*, *13*(1), 1–17.

Papadopoulos, K., T. Wallace, G. M. Milikh, W. Peter, and M. McCarrick (2005), The magnetic response of the ionosphere to pulsed HF heating, *Geophys. Res. Lett.*, *32*, L13101, doi:10.1029/2005GL023185.

Payne, J. A. (2007), Spatial structure of very low frequency modulated ionospheric currents, Ph.D. thesis, Stanford Univ., Stanford, Calif.

Payne, J. A., U. S. Inan, F. R. Foust, T. W. Chevalier, and T. F. Bell (2007), HF modulated ionospheric currents, *Geophys. Res. Lett.*, *34*, L23101, doi:10.1029/2007GL031724.

Peter, W. B., and U. S. Inan (2007), A quantitative comparison of lightning-induced electron precipitation and VLF signal perturbations, *J. Geophys. Res.*, *112*, A12212, doi:10.1029/2006JA012165.

Piddyachiy, D., U. S. Inan, and T. F. Bell (2008), DEMETER observations of an intense upgoing column of ELF/VLF radiation excited by the HAARP HF, *J. Geophys. Res.*, *113*, A10308, doi:10.1029/2008JA013208.

Platino, M., U. S. Inan, T. F. Bell, J. S. Pickett, E. J. Kennedy, J. G. Trotignon, J. L. Rauch, and P. Canu (2004), Cluster observations of ELF/VLF signals generated by modulated heating of the lower ionosphere with the HAARP HF transimitter, *Ann. Geophys.*, *22*, 2643–2653.

Platino, M., U. S. Inan, T. F. Bell, M. Parrot, and E. J. Kennedy (2006), DEMETER observations of ELF waves injected with the HAARP HF transmitter, *Geophys. Res. Lett.*, *33*, L16101, doi:10.1029/2006GL026462.

Raghuram, R., R. L. Smith, and T. F. Bell (1974), VLF antarctic antenna: Impedance and efficiency, *IEEE Trans. Antennas Propag.*, *22*, 334–338.

Rietveld, M. T., H. Kopka, and P. Stubbe (1986), D-region characteristics deduced from pulsed ionospheric heating under auroral elecrojet conditions, *J. Atmos. Terr. Phys.*, *48*(4), 311–326.

Rietveld, M. T., P. Stubbe, and H. Kopka (1989), On the frequency dependence of ELF/VLF waves produced by modulated ionospheric heating, *Radio Sci.*, *24*(3), 270–278.

Sazhin, S. S., and M. Hayakawa (1992), Magnetospheric chorus emissions: A review, *Planet. Space. Sci.*, *40*(5), 681–697.

Starks, M. J., R. A. Quinn, G. P. Ginet, J. M. Albert, G. S. Sales, B. W. Reinisch, and P. Song (2008), Illumination of the plasmasphere by terrestrial very low frequency transmitters: Model validation, *J. Geophys. Res.*, *113*, A09320, doi:10.1029/2008JA013112.

Stubbe, P., H. Kopka, and R. L. Dowden (1981), Generation of ELF and VLF waves by polar electrojet modulation: Experimental results, *J. Geophys. Res.*, *86*(A11), 9073–9078.

Tomko, A. A. (1981), Nonlinear phenomena arising from radio wave heating of the lower ionosphere, Ph.D. thesis, Penn. State Univ., University Park.

Yagitani, S., I. Nagano, K. Miyamura, and I. Kimura (1994), Full wave calculation of ELF/VLF propagation from a dipole source located in the lower ionosphere, *Radio Sci.*, *29*(1), 39–54.

M. B. Cohen, U. S. Inan, D. Piddyachiy, and N. G. Lehtinen, STAR Laboratory, Department of Electrical Engineering, Stanford University, 350 Serra Mall, Room 356, Stanford, CA 94305, USA. (mcohen@stanford.edu)

M. Gołkowski, Department of Electrical Engineering, University of Colorado Denver, 1200 Larimer St., Campus Box 110, Denver, CO 80204, USA.